RSC Advances

RSC Publishing

Preparation of Ag/α-Al₂O₃ for ethylene epoxidation through thermal decomposition assisted by extract of *Cinnamomum camphora*†

Daohua Sun,* Huixuan Wang, Genlei Zhang, Jiale Huang and Qingbiao Li*

An Ag/α-Al₂O₃ catalyst designed for application in the epoxidation of ethylene was prepared through thermal decomposition assisted by extract of *Cinnamomum camphora*. The effects of the reaction parameters on the catalytic performance were evaluated, including the extract concentration, calcining temperature and calcining time. The results demonstrated that the thermal decomposition should be conducted at 600 °C in N₂ for 60 min, assisted by 0.25 g mL⁻¹ *Cinnamomum camphora* extract. Compared with a simple thermal decomposition method, the sintering and aggregation of Ag particles and Ag loss during the reaction were alleviated by the presence of the catalyst that had been synthesized with the assistance of biomass.

1. Introduction

The epoxidation of ethylene is one of the most important industrial processes and has been studied extensively over the last 80 years. Silver is the only heterogeneous catalyst that can achieve reasonable selectivities for ethylene oxide (EO).[1] Factors including the type of Ag particle,[1,2] support materials,[3] and promoters[4] have been shown to affect catalyst performance. Currently, the most common method for the preparation of Ag catalysts is impregnation, where the Ag precursor is impregnated in the support and then reduced to Ag⁰ through thermal decomposition.[5–7] Thermal decomposition is a simple and efficient method for catalyst activation, but during this process, sintering and aggregation of Ag particles will generally occur when calcined over 200 °C,[8] which would seriously affect the dispersity of Ag particles on the support and therefore the performance of the Ag catalyst. Therefore, the thermal decomposition step has a pronounced effect on the catalytic performance of catalyst, and many studies have been dedicated to attempting to employ a more efficient activation method. One approach is to vary the atmosphere during calcination, using for example, superheated steam,[8] wet air (5% steam)[9] and a two stage atmosphere including the introduction of an inert atmosphere.[10] These methods partially alleviated the sintering of Ag

particles, but it was still difficult to better control the dispersity and size distribution due to the high temperatures involved. In addition, some researchers tried to introduce a reductant to decrease the decomposition temperature. For example, Akimi *et al.* prepared an Ag catalyst through the reduction of AgNO₃ by H₂ at a temperature of 250 °C.[11] But due to the presence of H₂, a higher cost and the necessity for greater protective measures are required for industrial operation. Besides H₂, other reductants such as hydrazine, formaldehyde, formic acid and low-carbon carboxylic acid amide have been studied.[12–15] However, the use of the above reductants may lead to security and environmental problems. Thus, the development of a safe and efficient approach to alleviate sintering and maintain the size and morphology of the Ag particles during the thermal decomposition is of significance.

Since Gardea-Torresdey[16] first reported the plant-mediated biosynthesis of gold nanoparticles, it has received increasing attention as an economical and eco-friendly alternative for the synthesis of nanomaterials.[17] With regard to silver, some studies[18–23] have reported the fabrication of Ag nanoparticles (AgNPs) by this method. Our group also obtained AgNPs with the use of the extract of *Cinnamomum camphora*[24] and *Cacumen platycladi*[25] leaves. AgNPs with a narrow size distribution and desired diameter can be obtained without any auxiliary surfactant or capping agent, owing to the presence of plant biomass that plays dual roles as both reductant and stabilizer. With the development of modern biological technology, we have a deeper understanding of the physical and chemical properties of biomass. If particular properties of biomass could be exploited in the field of catalysis, this would be an interesting concept. Our recent study[26] reported that the biosynthesized AuNPs immobilized onto a titanium silicalite-1 (TS-1) support maintained the same particle size without agglomeration, after

Department of Chemical and Biochemical Engineering, College of Chemistry and Chemical Engineering, Fujian Provincial Key Laboratory of Chemical Biology, Xiamen University, Xiamen, 361005, P. R. China. E-mail: sdaohua@xmu.edu.cn; Tel: +86 0592 2183088

† Electronic supplementary information (ESI) available: UV-Vis DRS spectra of Ag/α-Al₂O₃ calcined at 600 °C for different times, XRD patterns of Ag/α-Al₂O₃ catalysts with different concentrations of *C. camphora* leaf extract, SEM image and histogram of size distribution of Ag particles in Ag/α-Al₂O₃ catalysts prepared by the thermal decomposition method. See DOI: 10.1039/c3ra42336k

calcination at 375 °C. Moreover, excellent activity and high selectivity towards propylene epoxidation were achieved, partly because the residual biomass after calcination led to larger steric hindrance on the transfer of the active intermediate H_2O_2 from the gold to the Ti sites. In spite of these exact roles of biomass in the catalytic process, their detailed mechanisms remain unknown due to the complicated composition of the aqueous extract of plant biomass, the above result still inspired us to introduce biomass extract to the preparation of Ag/α-Al$_2$O$_3$ to attempt to solve the sintering problem during the thermal decomposition.

Herein, we report the preparation of Ag/α-Al$_2$O$_3$ through thermal decomposition assisted by extract of *Cinnamomum camphora* (*C. camphora*). The influence of preparation parameters on the catalytic activity in the epoxidation of ethylene were systematically investigated. The obtained Ag/α-Al$_2$O$_3$ catalysts were characterized using scanning electron microscopy (SEM), X-ray diffraction (XRD) and diffuse reflectance UV-Vis spectroscopy (UV-Vis DRS). Moreover, comparative studies on the catalytic performance were conducted between the catalyst prepared both with and without the extract of *C. camphora*.

2. Experimental

2.1. Preparation of *C. camphora* extract

The dried *C. camphora* leaves were crushed and then screened by a 20 mesh sieve. In order to obtain the *C. camphora* extract, 4.0 g biomass powder was carefully weighed and added to 400 mL DI water in a 500 mL conical flask. The mixture was then shaken at a rotation rate of 150 rpm for 10 h at 30 °C. The mixture was then filtered and the filtrate was retained for further experiments.

2.2. Preparation of Ag/α-Al$_2$O$_3$ catalysts

Ag/α-Al$_2$O$_3$ catalysts were prepared using the classical impregnation method.[27] In a typical synthesis of Ag/α-Al$_2$O$_3$ catalyst (15 wt% Ag loading), 0.1765 g of AgNO$_3$ was carefully weighed (Sinopharm Chemical Reagent Co. Ltd) and then dissolved in 1.2 mL of the *C. camphora* extract solution. This mixture was then supported on 1 g α-Al$_2$O$_3$ (20–40 mesh, Tianjin Chemical Research & Design Institute) at room temperature. Finally, having been dried at 50 °C in vacuum for 12 h, the obtained sample was calcined at 600 °C for 60 min in N$_2$.

2.3. Catalytic activity measurements

The catalytic tests were carried out in a fixed-bed stainless-steel reactor using a feed concentration of 15/7/5/73 vol% of C$_2$H$_4$/O$_2$/CO$_2$/N$_2$ and 0.5 mL catalyst at a space velocity of 7000 mL h^{-1} mL$_{cat}$$^{-1}$ and a reaction pressure of 2.0 ± 0.1 MPa. The temperature was measured by using a glass tube covered Cr–Al thermocouple located in the center of the catalyst bed. The concentrations of the reactant and the product were analyzed online by gas chromatographs (GC-950) equipped with thermal conductivity detectors (TCD) using a Porapak Q packed column (2 mm × 3 m), and a flame ionization detector (FID) using a β,β′-oxydipropionitrile/chromosorb 101 packed column

(2 mm × 1.5 m), respectively. The Porapak Q column was used to detect C$_2$H$_4$ and CO$_2$, while the β,β′-oxydipropionitrile column was used to detect EO.

2.4. Characterization of catalysts

XRD measurements were recorded on an X'Pert Pro X-ray Diffractometer (PANalytical BV, Netherlands) operated at a voltage of 40 kV and a current of 30 mA, with Cu Kα radiation. The UV-Vis DRS was performed on a Varian Cary-5000 spectrometer equipped with a diffuse-reflectance accessory, using dehydrated BaSO$_4$ as a reference in the range of 200–800 nm. SEM observations were carried out on a LEO-1530 Electron Microscope (LEO, Germany). The size distribution of the resulting NPs was estimated on the basis of SEM micrographs with the assistance of SigmaScan Pro software (SPSS Inc., Version 4.01.003). The actual Ag loadings of the samples were determined by atomic absorption spectroscopy (AAS).

3. Results and discussion

3.1. Influence of calcining temperature

The influence of the calcining temperature on the catalytic activity was investigated while the concentration of *C. camphora* leaf extract and the calcining time were set at 0.2 g mL^{-1} and 60 min, respectively. The activities of the Ag/α-Al$_2$O$_3$ catalysts calcined at 300, 400, 500, 600, and 700 °C are shown in Fig. 1. A very low EO concentration was found for catalysts calcined at 300 °C. The EO concentration increased as the temperature was increased from 400 to 600 °C, but declined slightly as the temperature was increased further to 700 °C. Therefore, a maximum EO concentration of 1.57% was obtained for the catalyst annealed at 600 °C. Under this condition, the EO selectivity is 74.59%, and the space time yield (STY) reaches 197.99 g h^{-1} L$_{cat}$$^{-1}$.

Fig. 2 displays the XRD patterns of Ag/α-Al$_2$O$_3$ catalysts calcined at different temperatures. When the calcining temperature was 300 °C, the diffraction peaks attributed to the unreacted silver salt or silver oxide were observed (peaks labelled *), which could explain the very low EO concentration obtained when using this catalyst. These peaks disappeared
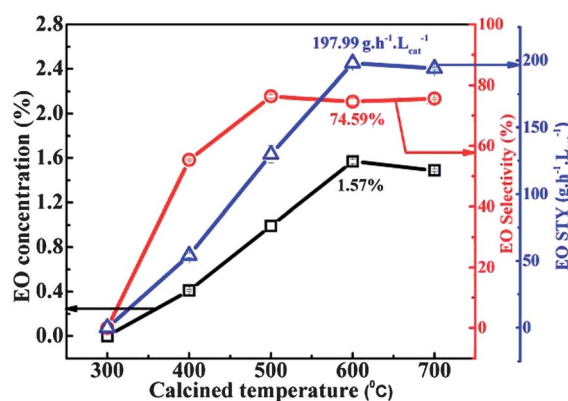

Fig. 1 Epoxidation of ethylene at 240 °C over Ag/α-Al$_2$O$_3$ catalysts calcined at different temperatures. □ EO concentration (%); ○ EO selectivity (%); △ EO STY (g h^{-1} L$_{cat}$$^{-1}$).
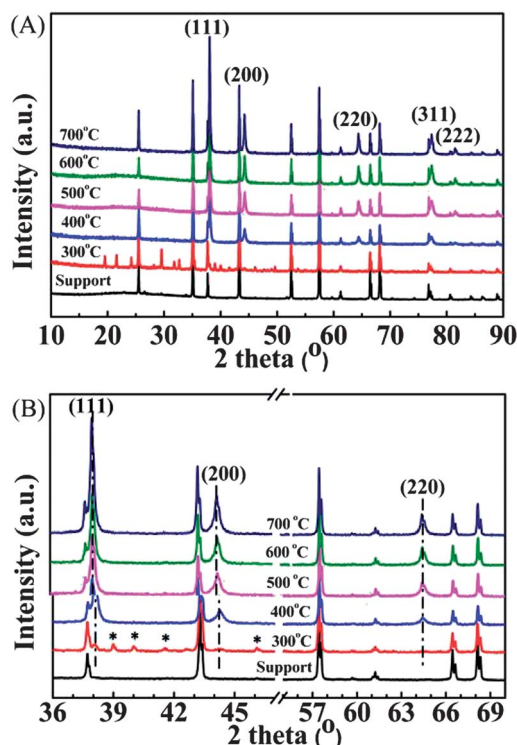
Fig. 2 XRD patterns of Ag/α-Al$_2$O$_3$ catalysts calcined at different temperatures.

when the catalyst was calcined at 400 °C and five diffraction peaks were detected which are ascribed to AgNPs. As the calcining temperatures were increased further, the Ag peaks became sharper, suggesting the formation of larger Ag particles.

It is generally recognized that UV-Vis DRS can be applied as an effective technique in the detection of the electronic states of silver in silver-based catalysts.[28,29] Fig. 3 displays the UV-Vis DRS spectra of Ag/α-Al$_2$O$_3$ calcined at different temperatures. The absorption band at around 350 nm corresponds to Ag^0 and the double peaks represent oxidized silver clusters (Ag$_n^{\delta+}$) which can be observed at 260 nm and 300 nm for this series of samples. These results can be explained by the presence of Ag NPs.[30] Strong absorptions at 205 nm associated with Ag$^+$ can be found in the
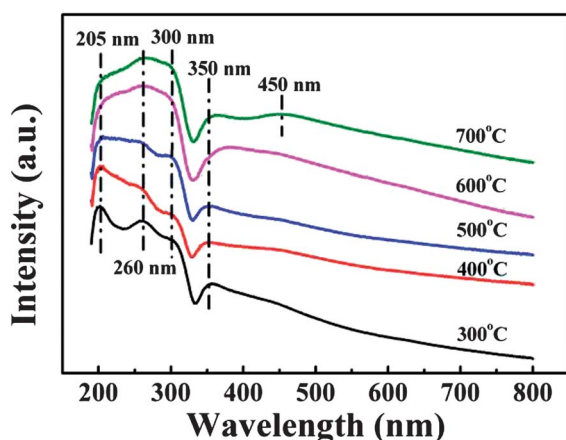
sample calcined at 300 °C, however, this peak gradually decreased in intensity as the calcining temperature was increased, until it finally disappeared at a calcining temperature of 600 °C. In view of the catalytic performances, Ag^0 and oxidized silver clusters (Ag$_n^{\delta+}$) are active species with respect to ethylene epoxidation, as opposed to Ag$^+$. Note that when the calcining temperature reached 700 °C, a new absorption band appeared at 450 nm, indicating that the nanoparticles had started to agglomerate.[31,32]

SEM images and corresponding histograms of the size distribution of the catalysts calcined at different temperatures are shown in Fig. 4. The spherical AgNPs were distributed on the surface of α-Al$_2$O$_3$ with a broader range of particle sizes. The average particle size increased significantly as the calcining temperature was increased. When the calcining temperatures were 300, 500, 600 and 700 °C, the obtained particle sizes of AgNPs were 35.7 ± 20.2, 137.1 ± 63.8, 239.8 ± 73.1 and 307.0 ± 140.1 nm, respectively. It should be noted that agglomeration had obviously occurred in the sample calcined at 700 °C.

From the above analysis, we can conclude that the determination of a suitable calcining temperature in a biomass-assisted thermal decomposition method is a viable strategy for obtaining catalysts with higher activities. The optimal catalytic performance was obtained for the catalyst calcined at 600 °C, because at this temperature, the silver species with higher valence states completely decomposed into Ag^0, leading to the formation of Ag particles with a uniform size distribution and a high dispersibility. Thus, 600 °C was chosen as the optimum calcining temperature.

3.2. Influence of calcining time

The activities of the Ag/α-Al$_2$O$_3$ calcined at 600 °C for 30, 60, 90 and 120 min are shown in Fig. 5. These catalysts all exhibited
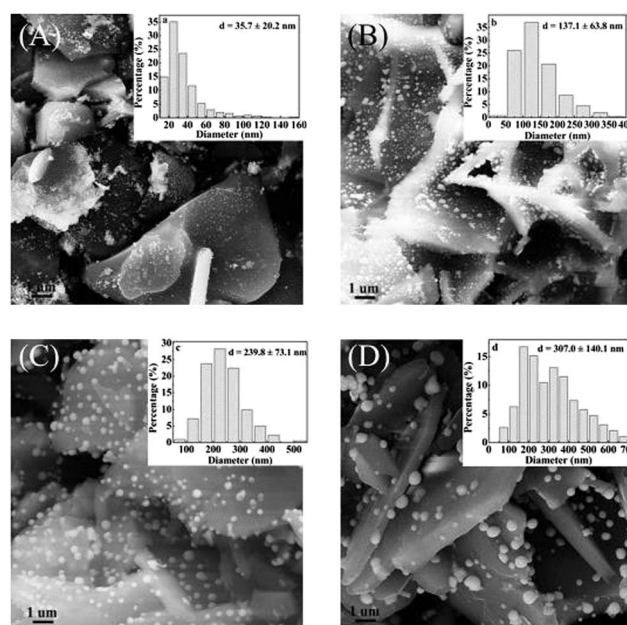

Fig. 4 SEM images (A–D) of Ag/α-Al$_2$O$_3$ catalysts with different calcining temperatures ((A) 300 °C; (B) 500 °C; (C) 600 °C; (D) 700 °C) and the corresponding histograms of Ag particle size distribution (insets A–D).

Fig. 3 UV-Vis DRS spectra of Ag/α-Al$_2$O$_3$ calcined at different temperatures.

the desired catalytic activity, giving rise to EO concentrations higher than 1.3% and EO selectivities of above 70%. The maximum conversion of ethylene was achieved by the catalyst which was calcined for 60 min. Using this catalyst, the obtained EO concentration was 1.57% and the EO selectivity was 74.59%. The quality of the Ag/α-Al$_2$O$_3$ catalyst samples was further determined by UV-Vis DRS (Fig. S1†). The strong absorption bands of Ag^0 and Ag$_n^{\delta+}$ can be observed in every spectrum, and the absorption band at around 205 nm assigned to Ag$^+$ was absent for all of the catalysts. However, when the calcining time was extended to 120 min, a weak characteristic absorption band at 460 nm appeared, indicating partial agglomeration of the silver nanoparticles.

3.3. Influence of *C. camphora* leaf extract concentration

The above results demonstrate that the optimal thermal decomposition temperature and time are 600 °C in N$_2$ and 60 min, respectively. The effect of the *C. camphora* leaf extract concentration (0.05, 0.10, 0.15, 0.20, 0.25 and 0.30 g mL^{-1}) on the catalytic activity with a silver loading of 15% and a reaction temperature of 240 °C, are shown in Fig. 6. As the concentration of *C. camphora* leaf extract was increased, the EO concentration also increased from 0.47% to 1.65%, before decreasing to 1.50%. A maximum in the selectivity of EO of 77% was obtained when the concentration of *C. camphora* leaf extract was 0.05 g mL^{-1}, however, the obtained EO concentration was not desirable and the STY of EO was lower in this case. Considering both the EO concentration and the selectivity of EO, the optimal concentration of the *C. camphora* leaf extract was found to be 0.25 g mL^{-1}, and the catalyst prepared with this concentration gave rise to an EO concentration of 1.65%, a selectivity of 75.31% and a STY of 211.48 g h^{-1} L$_{cat}^{-1}$ at 240 °C.

XRD patterns of Ag/α-Al$_2$O$_3$ made using different concentrations of *C. camphora* leaf extract (Fig. S2†) possessed five obvious diffraction peaks attributable to the Ag^0 species, and no other miscellaneous peaks were observed for any of the samples. This proves that the AgNO$_3$ had completely decomposed and that no Ag$_x$O was present when the catalyst was activated at 600 °C in N$_2$.
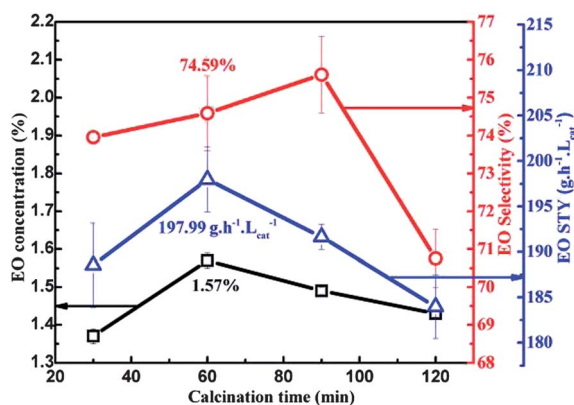

Fig. 6 Epoxidation of ethylene at 240 °C over Ag/α-Al$_2$O$_3$ catalysts treated with different concentrations of *C. camphora* leaf extract. □ EO concentration (%); ○ EO selectivity (%); △ EO STY (g h^{-1} L$_{cat}^{-1}$).

It is interesting that with the increase of *C. camphora* leaf extract concentration, the peaks representing Ag^0 tended to broaden, which demonstrates that the sizes of the resulting Ag particles were decreasing. This phenomenon was further verified by the SEM images of the catalysts shown in Fig. 7. As the concentration of extract was increased, the particle diameter of the silver particles decreased gradually from 727.0 ± 321.7 nm (at 0.05 g mL^{-1}) to 110.3 ± 41.2 nm (at 0.30 g mL^{-1}). Therefore, in the preparation of the Ag/α-Al$_2$O$_3$ catalysts through a biomass-assisted thermal decomposition process, the utilization of

Fig. 7 SEM images and histograms of size distribution (insets) of the Ag/α-Al$_2$O$_3$ catalysts treated with different concentrations of *C. camphora* leaf extract: (A) 0.05, (B) 0.10, (C) 0.15, (D) 0.20, (E) 0.25 and (F) 0.30 g mL^{-1}.

Fig. 5 Epoxidation of ethylene at 240 °C over Ag/α-Al$_2$O$_3$ catalysts calcined at 600 °C for different times. □ EO concentration (%); ○ EO selectivity (%); △ EO STY (g h^{-1} L$_{cat}^{-1}$).

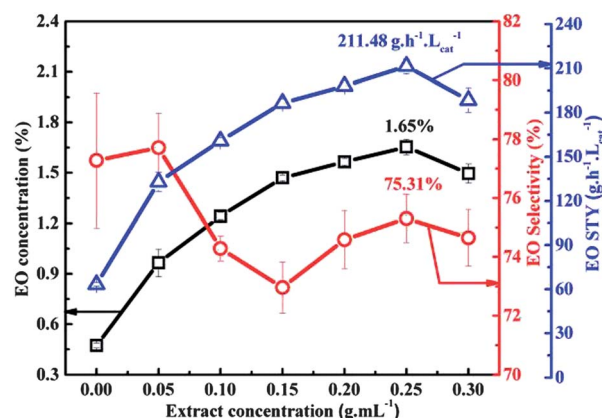*C. camphora* extract retards the growth of the AgNPs in the thermal decomposition process at high temperature. The use of an appropriate amount of *C. camphora* extract in this process is beneficial to the performance of the resulting catalyst.

3.4. Comparison of the performance of the Ag/α-Al₂O₃ catalysts prepared by traditional and biomass-assisted thermal decomposition methods

The comparative studies were performed with two catalysts, one prepared by a thermal decomposition method (catalyst A), and the other by a biomass-assisted thermal decomposition method (catalyst B). Both catalysts were otherwise prepared by the same procedure, using calcining conditions of 600 °C in N_2 for 60 min, and a silver loading of 15%. The only difference was that 0.25 g mL^{-1} of *C. camphora* leaf extract was introduced during the thermal decomposition of catalyst B. As can be seen from Table 1, the performance of catalyst B was better than that of catalyst A. More specifically, at a reaction temperature of 240 °C, the use of catalyst B resulted in an EO concentration of 1.65%, an EO selectivity of 75.31% and a STY of 211.48 g h^{-1} L$_{cat}$$^{-1}$, while catalyst A resulted in an EO concentration of 0.47%, an EO selectivity of 77.28% and a STY 63.32 g h^{-1} L$_{cat}$$^{-1}$. In the reaction with catalyst B, as the reaction temperature was increased, the concentration of EO increased gradually but there was a decline in selectivity. When the reaction temperature was increased to 260 °C, the concentration, selectivity and STY of EO were 2.08%, 65.47% and 268.92 g h^{-1} L$_{cat}$$^{-1}$, respectively. It is worth mentioning that in this work, the most common and facile Ag precursor ($AgNO_3$) and support (α-Al₂O₃) were employed, and no promoter or any additives were involved. van Santen[33] *et al.* reported that the EO selectivity of un-promoted metallic silver is around 50%, though the catalytic performance can be enhanced by the addition of alkali compounds as promoters, or ppm quantities of chlorine, in the form of chlorinated hydrocarbons, in to the feed stream. SEM images of catalyst A (Fig. S3†) show that the Ag particles were distributed unevenly on the carrier surface, and that there were numerous particles with a large size, *i.e.* that agglomeration had occurred during the thermal decomposition. The UV-Vis DRS spectra shown in Fig. 8 verified this result. An obvious absorption band at 450 nm associated with the agglomeration of silver particles can easily be observed in the spectrum of catalyst A, while this peak is absent in the spectrum of catalyst B. This could explain the poorer performance of catalyst A.

Moreover, the actual silver loading of the two catalysts, both before and after the reaction, were determined by AAS. For catalyst A, the actual loading of silver decreased from 14.52% to 6.03%, therefore there was a 58.47% loss of Ag after the catalyst test. However, for catalyst B, the Ag loading decreased slightly from 14.76% to 13.79% equating to only a 7.95% loss of Ag after the reaction. This could be due to the control over the size of the Ag particles that results from the introduction of the biomass, therefore reducing sintering aggregation and enhancing the interaction between the Ag particles and the support. During the catalytic process, the loss of the Ag component led to Ag enrichment in the tail area of the catalytic bed, which resulted in a vigorous reaction in this region, and a corresponding severe drop in the EO selectivity.

Therefore, it can be inferred that the Ag particles in the Ag/α-Al₂O₃ catalyst prepared by traditional thermal decomposition tended to agglomerate during the thermal decomposition. This agglomeration behavior had a negative impact on the catalytic ability in the following ways: first, the activity of the catalyst was reduced due to the decrease in the surface area of the active component. Additionally, the binding affinity between the silver particles and the carrier was significantly reduced, therefore
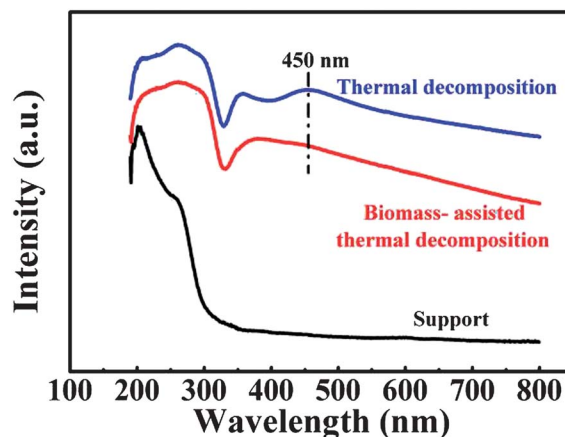

Fig. 8 UV-Vis DRS spectra of Ag/α-Al₂O₃ catalysts prepared by a thermal decomposition method and a biomass-assisted thermal decomposition method.

Table 1 Epoxidation of ethylene over Ag/α-Al₂O₃ catalysts prepared by a thermal decomposition method and a biomass-assisted thermal decomposition method[a]

Catalyst	Method	Reaction temperature (°C)	EO concentration (%)	EO selectivity (%)	EO space time yield (g h^{-1} L$_{cat}$$^{-1}$)
A	Thermal decomposition without biomass	240	0.47 ± 0.02	77.28 ± 2.29	63.32 ± 1.22
		250	0.89 ± 0.03	70.34 ± 1.78	109.20 ± 3.40
		260	1.27 ± 0.02	61.83 ± 1.68	169.15 ± 3.35
		280	0.65 ± 0.06	21.70 ± 1.45	84.49 ± 6.81
B	Biomass-assisted thermal decomposition	225	1.21 ± 0.04	81.95 ± 1.14	161.09 ± 4.30
		240	1.65 ± 0.05	75.31 ± 0.82	211.48 ± 4.97
		250	1.89 ± 0.07	70.27 ± 1.44	252.04 ± 8.40
		260	2.08 ± 0.02	65.47 ± 0.76	268.92 ± 4.26

[a] *Reaction conditions:* feed gas $V(C_2H_4) : V(O_2) : V(CO_2) : V(N_2) = 15 : 7 : 5 : 73$, reaction pressure = 2 MPa, GHSV = 7000 mL h^{-1} mL$_{cat}$$^{-1}$.

hindering the effective transfer of electrons. Ag particles also easily fell off the support, resulting in a serious loss of precious metal (Ag). As has been demonstrated, a high dispersity of Ag particles and therefore a catalyst with a high Ag loading, is difficult to achieve on the α-Al$_2$O$_3$ support with a low specific surface area using the traditional thermal decomposition process.[14] However, when biomass-assisted thermal decomposition methods were employed, the biomass affected the crystal growth process of the Ag particles. The excellent activity and high selectivity of the Ag/α-Al$_2$O$_3$ catalysts employed at a relatively high reaction temperature should be attributed to the existence of residual biomolecules on the catalyst, supposedly preventing the agglomeration of the AgNPs and strengthening their interaction with the carrier. Thus the probability and rate of Ag particle agglomeration are reduced dramatically.

4. Conclusions

In summary, we have reported a novel method to prepare a Ag/α-Al$_2$O$_3$ catalyst for the epoxidation of ethylene through biomass-assisted thermal decomposition. Effects of parameters including calcining temperature, calcining time and *C. camphora* extract concentration, on the catalytic performance have been evaluated. The optimal thermal decomposition conditions were found to be 600 °C in N$_2$ for 60 min, assisted by 0.25 g mL^{-1} *C. campora* extract. The catalyst prepared using these conditions resulted in an EO concentration of 1.65%, an EO selectivity of 75.31% and a space time yield of 211.48 g h^{-1} L$_{cat}$$^{-1}$ at 240 °C. The performance of the as-prepared catalyst was better than its analogue, prepared by a simple thermal decomposition method, because the introduction of biomass contributed to the effective control of the Ag particle size, reducing sintering aggregation during the thermal decomposition process and enhancing the interaction between the silver particles and the carrier. This method could be an effective technique to alleviate sintering during thermal decomposition, and to improve the potential performance of catalysts with a high metal loading.

Acknowledgements

References

1 P. Christopher and S. Linic, *J. Am. Chem. Soc.*, 2008, **130**, 11264.
2 P. Christopher and S. Linic, *ChemCatChem*, 2010, **2**, 78.
3 A. Chongterdtoonsku, J. W. Schwank and S. Chavade, *J. Mol. Catal. A: Chem.*, 2012, **358**, 58.
4 M. O. Ozbek, I. Onal and R. A. van Santen, *ChemCatChem*, 2013, **5**, 443.
5 M. A. Pena, D. M. Carr, K. L. Yeung and A. Varma, *Chem. Eng. Sci.*, 1998, **53**, 3821.
6 A. Takahashi, N. Hamakawa, I. Nakamura and T. Fujitani, *Appl. Catal., A*, 2005, **294**, 34.
7 M. C. N. Amorim de Carvalho, F. B. Passos and M. Schmal, *J. Catal.*, 2007, **248**, 124.
8 N. Nojiri and Y. Sakai, Silver catalyst for production of ethylene oxide from ethylene, *US Pat.* 4786624, 1988.
9 A. Bortinger and A. D. Sehmitz, Activation of high selectivity ethylene oxide catalyst, *US Pat.* 0225511A1, 2007.
10 V. S. Bhise, A. Bortinger and S. R. Allen, Two-stage calcinations for catalyst production, *US Pat.* 0039316AI, 2008.
11 A. Ayame, Y. Uchida, H. Ono, M. Miyamoto, T. Sato and H. Hayasaka, *Appl. Catal., A*, 2003, **244**, 59.
12 J. C. Dellamorte, J. Lauterbach and M. A. Barteau, *Catal. Today*, 2007, **120**, 182.
13 M. V. Badani and M. A. Vannice, *Appl. Catal., A*, 2000, **204**, 129.
14 C. Maldonado, J. L. G. Fierro, G. Birke, E. Martinez and P. Reyes, *J. Chil. Chem. Soc.*, 2010, **55**, 506.
15 A. N. Pestryakov, *Catal. Today*, 1996, **28**, 239.
16 J. L. Gardea-Torresdey, J. G. Parsons, E. Gomez, J. Peralta-Videa, H. E. Troiani, P. Santiago and M. Jose Yacaman, *Nano Lett.*, 2002, **2**, 397.
17 A. K. Mittal, Y. Chisti and U. C. Banerjee, *Biotechnol. Adv.*, 2013, **31**, 346.
18 J. Y. Song and B. S. Kim, *Bioprocess Biosyst. Eng.*, 2009, **32**, 79.
19 J. L. Gardea-Torresdey, E. Gomez, J. R. Peralta-Videa, J. G. Parsons, H. Troiani and M. Jose-Yacaman, *Langmuir*, 2003, **19**, 1357.
20 S. S. Shankar, A. Ahmad and M. Sastry, *Biotechnol. Prog.*, 2003, **19**, 1627.
21 C. Krishnaraj, E. G. Jagan, S. Rajasekar, P. Selvakumar, P. T. Kalaichelvan and N. Mohan, *Colloids Surf., B*, 2010, **76**, 50.
22 D. Philip, *Spectrochim. Acta, Part A*, 2011, **78**, 327.
23 S. S. Shankar, A. Rai, A. Ahmad and M. Sastry, *J. Colloid Interface Sci.*, 2004, **275**, 496.
24 J. L. Huang, L. Q. Lin, Q. B. Li, D. H. Sun, Y. P. Wang, Y. H. Lu, N. He, K. Yang, X. Yang, H. X. Wang, W. T. Wang and W. S. Lin, *Ind. Eng. Chem. Res.*, 2008, **47**, 6081.
25 J. L. Huang, G. W. Zhan, B. Y. Zheng, D. H. Sun, F. F. Lu, Y. Lin, H. M. Chen, Z. D. Zheng, Y. M. Zheng and Q. B. Li, *Ind. Eng. Chem. Res.*, 2011, **50**, 9095.
26 M. M. Du, G. W. Zhan, X. Yang, H. X. Wang, W. S. Lin, Y. Zhou, J. Zhu, L. Ling, J. L. Huang, D. H. Sun, L. S. Jia and Q. B. Li, *J. Catal.*, 2011, **283**, 192.
27 A. Musi, P. Massiani, D. Brouri, J. M. Trichard and P. Da Costa, *Catal. Lett.*, 2009, **128**, 25.
28 X. She and M. Flytzani-Stephanopoulos, *J. Catal.*, 2006, **237**, 79.
29 S. G. Aspromonte, R. M. Serra, E. E. Miró and A. V. Boix, *Appl. Catal., A*, 2011, **407**, 134.
30 L. Zhang, C. B. Zhang and H. He, *J. Catal.*, 2009, **261**, 101.
31 A. Keshavaraja, X. She and M. Flytzani-Stephanopoulos, *Appl. Catal., B*, 2000, **27**, L1–L9.
32 A. N. Pestryakov and A. A. Davydov, *J. Electron Spectrosc. Relat. Phenom.*, 1995, **74**, 195.
33 M. O. Ozbek and R. A. van Santen, *Catal. Lett.*, 2013, **143**, 131.